

1

2

3

4

5

6

7

8

9

10                   Supplementary Material (ESI) for Journal of Materials Chemistry A

11                   This journal is (c) The Royal Society of Chemistry 2013

12

13                   **Synthesis, characterization and application of**  
14                   **lanthanum-impregnated activated alumina for F removal**

15

16                   **Qiantao Shi<sup>a</sup>, Yuying Huang<sup>b</sup> and Chuanyong Jing<sup>\*a</sup>**

17

18

19

20                   *<sup>a</sup>State Key Laboratory of Environmental Chemistry and Ecotoxicology, Research Center for*  
21                   *Eco-Environmental Science, Chinese Academy of Science, Beijing 100085, China. Fax: 010*  
22                   *62849523; Tel: 010 62849523; E-mail: [cjing@rcees.ac.cn](mailto:cjing@rcees.ac.cn)*

23                   *<sup>b</sup>Shanghai Synchrotron Radiation Facility, Shanghai Institute of Applied Physics, Chinese*  
24                   *Academy of Sciences, Shanghai 201214, China*

25

26

27

28

Supplementary Material (ESI) for Journal of Materials Chemistry A

29

This journal is (c) The Royal Society of Chemistry 2013

30

31

32



33

34

35

36

37

38

39

40

**Fig. S1** Photos of AA,LAA and LaOOH.

41

42

43

44

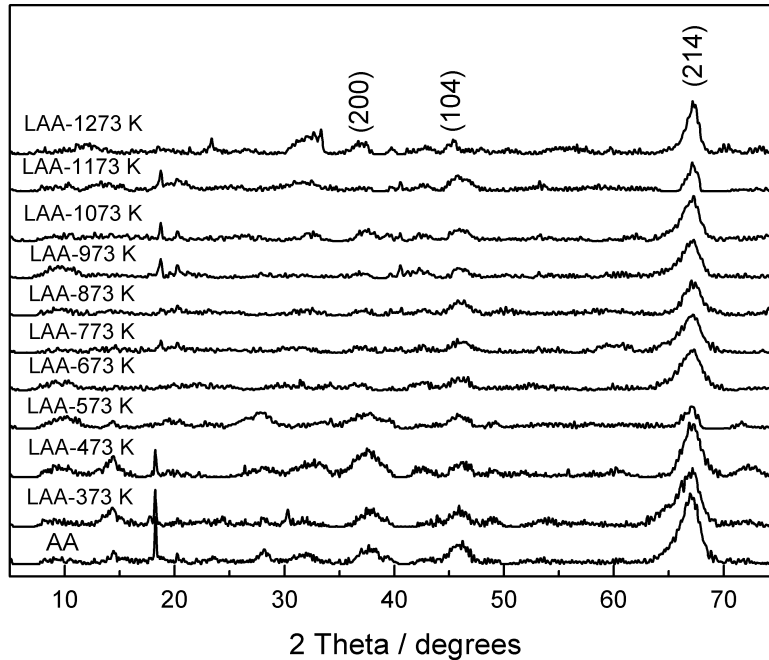
45

Supplementary Material (ESI) for Journal of Materials Chemistry A

46

This journal is (c) The Royal Society of Chemistry 2013

47



62

63 **Fig. S2** XRD patterns of various LAAs synthesized at different calcination temperatures  
( $\chi$ -Al<sub>2</sub>O<sub>3</sub>PDF No. 13-0373).

64

65 The XRD results suggested that there were no new crystals in LAA compared  
66 with AA. The results indicated that LaOOH supported on LAA were amorphous. This  
67 result is inline with our previous work<sup>1</sup>. The characterization peaks of Al<sub>2</sub>O<sub>3</sub> were  
68 weaker upon LaOOH impregnation, indicating that Al<sub>2</sub>O<sub>3</sub> was covered by LaOOH.  
69

70

71

72

73                   Supplementary Material (ESI) for Journal of Materials Chemistry A

74                   This journal is (c) The Royal Society of Chemistry 2013

75

76   **Table S1.** Pore volume and diameter of AA and LAA.

	Pore volume (mL g <sup>-1</sup> )	Pore diameter of micropore (nm)	Pore diameter of mesopore (nm)
<b>AA</b>	0.4485	0.588	3.94
<b>LAA</b>	0.3038	0.488	3.706

77

78

79

Supplementary Material (ESI) for Journal of Materials Chemistry A

80

This journal is (c) The Royal Society of Chemistry 2013

81

82

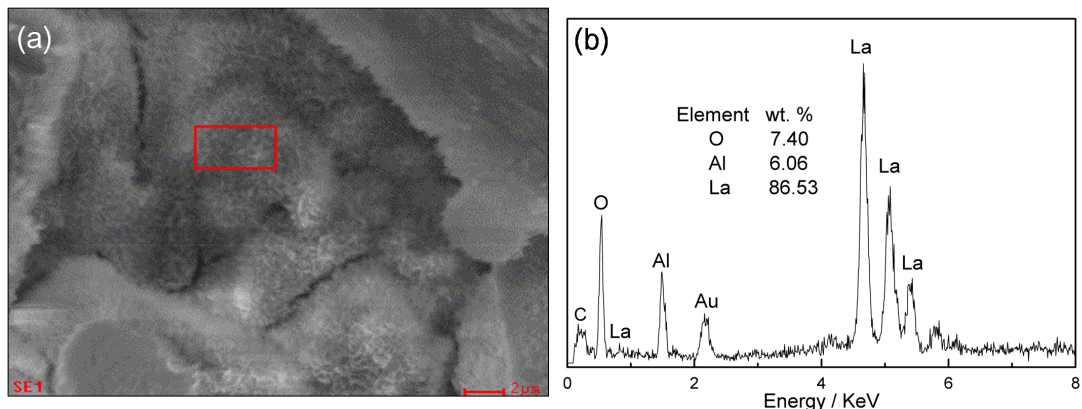


Fig. S3 EDS of flake structures on LAA.

93

94

95

96

97

Supplementary Material (ESI) for Journal of Materials Chemistry A

98

This journal is (c) The Royal Society of Chemistry 2013

99

100

101

102

103

104

105

106

107

108

109

110

111

112

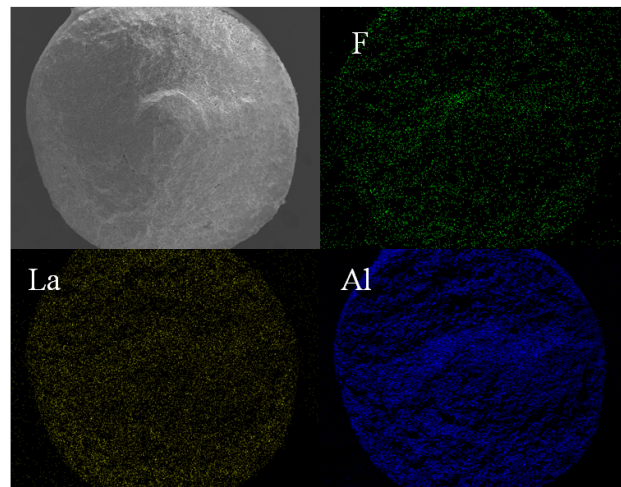


**Fig. S4** EDS elemental mapping of F, La, and Al on LAA adsorbed with F.

113

114

115

116

117

Supplementary Material (ESI) for Journal of Materials Chemistry A

118

This journal is (c) The Royal Society of Chemistry 2013

119

120

121

122

123

124

125

126

127

128

129

130

131

132

133

134

135

136

137

138

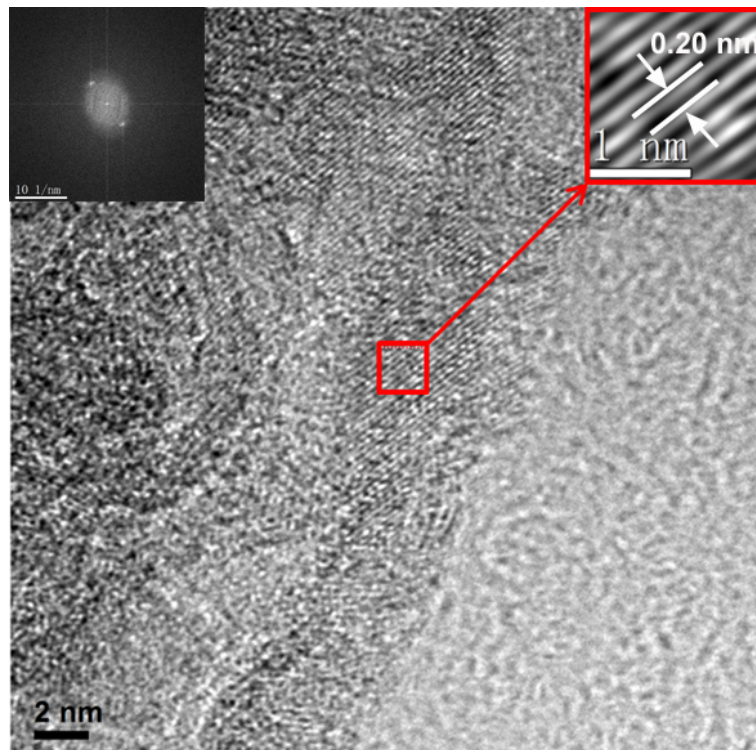


**Fig. S5** High resolution transmission electron microscope HRTEM of LAA.

139

140 As shown in Fig. S4, the only interplanar distance we found in LAA is 1.98 Å ( $\approx$   
141 0.20 nm), corresponding to  $\gamma$ -Al<sub>2</sub>O<sub>3</sub> (1 0 4) (PDF No. 13-0373) in our XRD results.

142 The XRD and HRTEM results showed that there is no crystalline form of La<sub>2</sub>O<sub>3</sub>,  
143 LaOOH or LaAlO<sub>3</sub> in LAA, suggesting that the lanthanum oxides supported on LAA  
144 are amorphous. This result is in agreement with our previous work<sup>1</sup>.

145

Supplementary Material (ESI) for Journal of Materials Chemistry A  
This journal is (c) The Royal Society of Chemistry 2013

## 149 EXAFS Data collection

The La LIII-edge spectra were collected at beamline 14W1 of the Shanghai Synchrotron Radiation Facility (SSRF), China. The spectra were taken under standard SSRF operation conditions (2.8 GeV and 150-280 mA) with a double-crystal Si (111) monochromator. The spectra were collected with a fluorescence detector positioned at a 90° angle to the incident beam at room temperature. Three scans were collected from each sample, inspected for overall quality and averaged to improve the signal/noise ratio.

EXAFS data analysis was performed using the ATHENA and ATEMIS program in the IFEFFIT computer package.<sup>2,3</sup> The analysis procedure was similar to our previous studies.<sup>4,5</sup> The raw data measured in intensities were converted to  $\mu(E)$ , and averaged spectra were used in the analysis. The EXAFS signal  $\chi(k)$  was extracted from the measured data using the AUTOBK algorithm<sup>6</sup> where  $k$  is the photoelectron wave number. The primary quantity for EXAFS is then  $\chi(k)$ , the oscillations as a function of photoelectron wave number.  $\chi(k)$  was weighted by  $k^2$  to account for the dampening of oscillations with increasing  $k$ . The different frequencies in the oscillations in  $\chi(k)$  correspond to different near neighbor coordination shells which can be described and modeled according to the EXAFS equation

$$167 \quad \chi(k) = \sum_j \frac{N_j f_j(k) e^{-2k^2 \sigma_j^2}}{k R_j^2} \sin[2kR_j + \delta_j(k)]$$

where  $f(k)$  and  $\delta(k)$  represent the photoelectron backscattering amplitude and phase shift, respectively,  $N$  is the number of neighboring atoms,  $R$  is the distance to the neighboring atom, and the  $\sigma^2$  is the Debye-Waller factor representing the disorder in the neighbor distance. The  $k^2$  weighted EXAFS in k-space ( $\text{\AA}^{-1}$ ) was Fourier transformed (FT) in R-space ( $\text{\AA}$ ). The experimental spectra were fitted with single-scattering theoretical phase-shift and amplitude functions calculated with the *ab initio* computer code FEFF6<sup>7</sup> using atomic clusters generated from the crystal structure of  $\alpha\text{-La}_2\text{O}_3$  and SrLa (AlO<sub>4</sub>). The many-body amplitude reduction factor ( $S_0^{-2}$ ) was established as 0.78 by isolating and fitting the first-shell La-O of LaOOH spectrum. The spectrum was fit by first isolating and fitting the first-shell La-O to estimate  $\Delta E_0$ , the difference in threshold energy between theory and experiment. Then  $\Delta E_0$  was fixed to the best fit value from first-shell fitting and kept the same for all interatomic shells in a given spectrum. In addition, the  $\Delta E_0$  value was allowed to float by no more than  $\pm 10$  eV. The parameters such as interatomic distance ( $R$ ), coordination number (CN), and Debye-Waller factor ( $\sigma^2$ ) were first established with reasonable guesses and were fitted in R-space. The error in the overall fits was determined using R-factor, the goodness-of-fit parameter:  $R\text{-factor} = \Sigma(\chi_{\text{data}} - \chi_{\text{fit}})^2 / \Sigma(\chi_{\text{data}})^2$ . Good fits occur for R-factor < 0.05.

186

187

188

Supplementary Material (ESI) for Journal of Materials Chemistry A

189

This journal is (c) The Royal Society of Chemistry 2013

190

191

**Table S2** Structure parameters derived from La L<sub>III</sub>-edge EXAFS analysis.

Sample	shell	CN <sup>a</sup>	R (Å) <sup>b</sup>	$\sigma^2$ (Å <sup>2</sup> ) <sup>c</sup>	$\Delta E_0$ (eV) <sup>d</sup>	R-factor <sup>e</sup>
	La-O	7.6 ± 2.2	2.58 ± 0.04	0.010 ± 0.008		
LaOOH	La-O	1.0 ± 0.2	3.56 ± 0.34	0.016 ± 0.007	6.75	0.028
	La-La	3.3 ± 1.4	4.22 ± 0.07	0.031 ± 0.012		
	La-O	7.7 ± 1.4	2.56 ± 0.06	0.007 ± 0.003		
LAA	La-Al	3.7 ± 1.2	3.19 ± 0.12	0.018 ± 0.010		
	La-La	3.5 ± 1.5	3.43 ± 0.16	0.028 ± 0.013	2.36	0.012
	La-La	4.3 ± 1.4	4.12 ± 0.18	0.033 ± 0.015		

192

193

<sup>a</sup> coordination number. <sup>b</sup>interatomic distance. <sup>c</sup>Debye-Waller factor. <sup>d</sup> threshold energy shift. <sup>e</sup> goodness-of-fit parameter: R-factor =  $\Sigma(\chi_{\text{data}} - \chi_{\text{fit}})^2 / \Sigma(\chi_{\text{data}})^2$

194

195

196

Supplementary Material (ESI) for Journal of Materials Chemistry A

197

This journal is (c) The Royal Society of Chemistry 2013

198

199

200

201

202

203

204

205

206

207

208

209

210

211

212

213

214

215

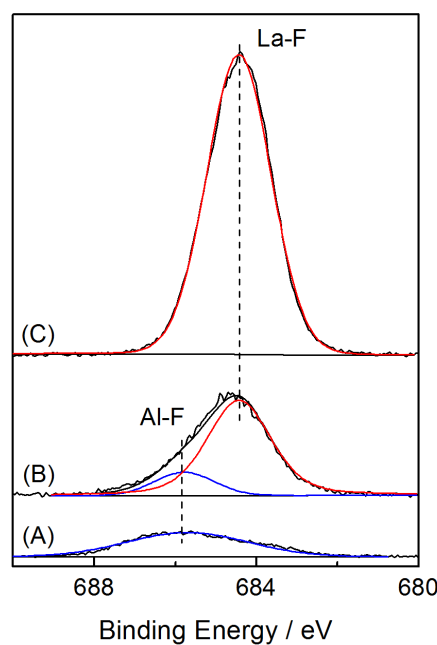


**Fig. S6** High resolution XPS surveys of F 1s for spent AA (A), LAA (B), and LaOOH (C) Vertical lines indicate Al-F (blue) and La-F (red) at  $685.7 \pm 0.1$  eV and  $684.4 \pm 0.1$  eV, respectively.

216

The high resolution XPS surveys of F 1s for spent AA, LAA and LaOOH were used to explore the F adsorption on the adsorbents. The F 1s spectra were simulated by considering two peaks from Al-F and La-F.<sup>8,9</sup> The peak position of Al-F at 685.7 eV was observed in AA and LAA. Moreover, the peak of La-F at 684.4 eV was resolved in LaOOH and LAA.

217

218

219

220

221

222

223

224

225

226

227

228

Supplementary Material (ESI) for Journal of Materials Chemistry A

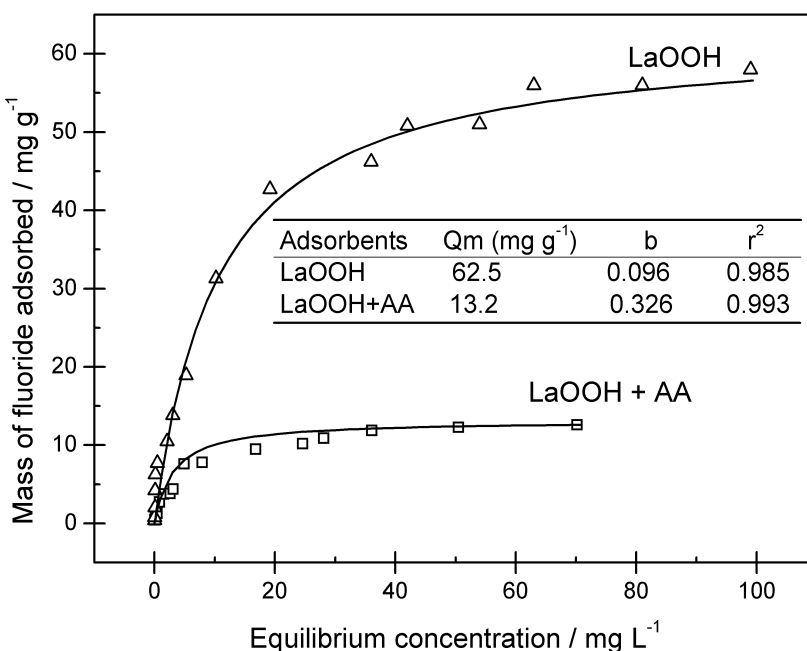
229

This journal is (c) The Royal Society of Chemistry 2013

230

231

232



233

234

235

236

237

238

239

240

241

242

243

244

245

246

247

248

249

**Fig. S7** F desorption isotherms on LaOOH and the mixture of AA and LaOOH (with 20 wt.% La). Adsorbent = 1 g L<sup>-1</sup>, pH = 7, Temperature = 298 ± 2 K. Inset Table: Langmuir parameters: Qm is the maximum adsorption amount (mg g<sup>-1</sup>), b is Langmuir constant (L mol<sup>-1</sup>), and r<sup>2</sup> is the correlation coefficient.

250

251

252

253

As shown in Fig. S7, the F adsorption capacity of the mixture of AA and LaOOH (13.2 mg g<sup>-1</sup>) is no better than that of LAA (16.9 mg g<sup>-1</sup>, Figure 9). In this experiment, the weight percentage of La in the mixture was the same as that in LAA (Fig. 2). The results indicate that LAA takes the advantage of porous AA to anchor the LaOOH flakes, which resulted in uniformly distributed LaOOH for F adsorption. Conversely, the LaOOH powder may aggregate in the solution and less active sites are available for effective F adsorption.

254

255

256

257

258

259

260

261

262

263

264

265

266

267

In addition, the average particle size of LaOOH was 702.0 ~742.1 nm as determined using a Zetasizer Nano ZS (Malvern Instrument, UK). This small particle size indicates that the LaOOH should have difficulties in the solid/liquid separation and recovery from the treated water. In contrast, LAA was synthesized based on a commercial AA granule with a diameter of 1~3 mm (Fig. S1). This granule is suitable for column water treatment in the large scale.

268

Supplementary Material (ESI) for Journal of Materials Chemistry A

269

This journal is (c) The Royal Society of Chemistry 2013

270

271

272

273

274

275

276

277

278

279

280

281

282

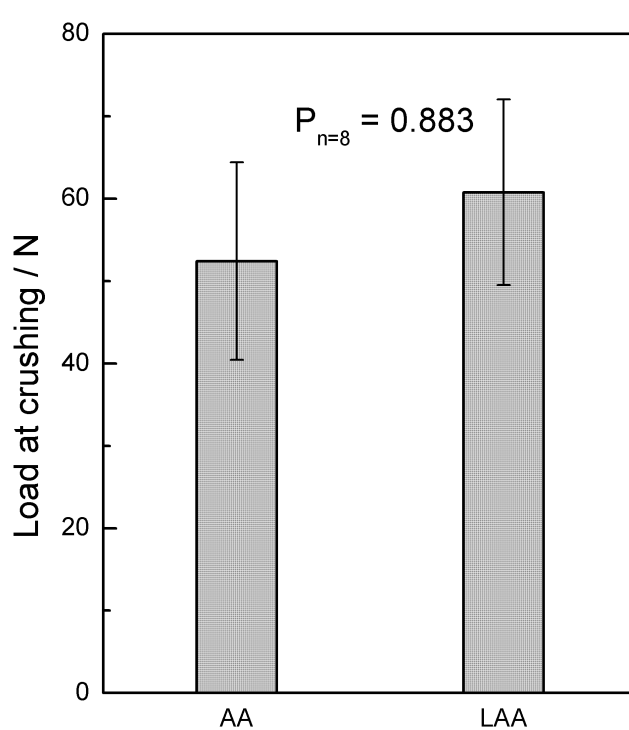
283

284

285

286

287



288

### Adsorbents

289

**Fig. S8** Mechanical strength of AA and LAA.

290

291 The mechanical strength of AA and LAA were analyzed using a universal testing  
292 machine at a cross-head speed of  $2 \text{ mm min}^{-1}$  (Sansi Inc., China). The loads at  
293 crushing for AA and LAA were  $52.4 \pm 12.0$  and  $60.8 \pm 11.3$  N, respectively. No  
294 significant difference existed between AA and LAA ( $p=0.883$ ,  $n=8$ , Fig. S8). The  
295 good mechanical strength implies that LAA can be used in the large scale and be  
296 easily recovered from treated water.

297

298

299

Supplementary Material (ESI) for Journal of Materials Chemistry A

300

This journal is (c) The Royal Society of Chemistry 2013

301

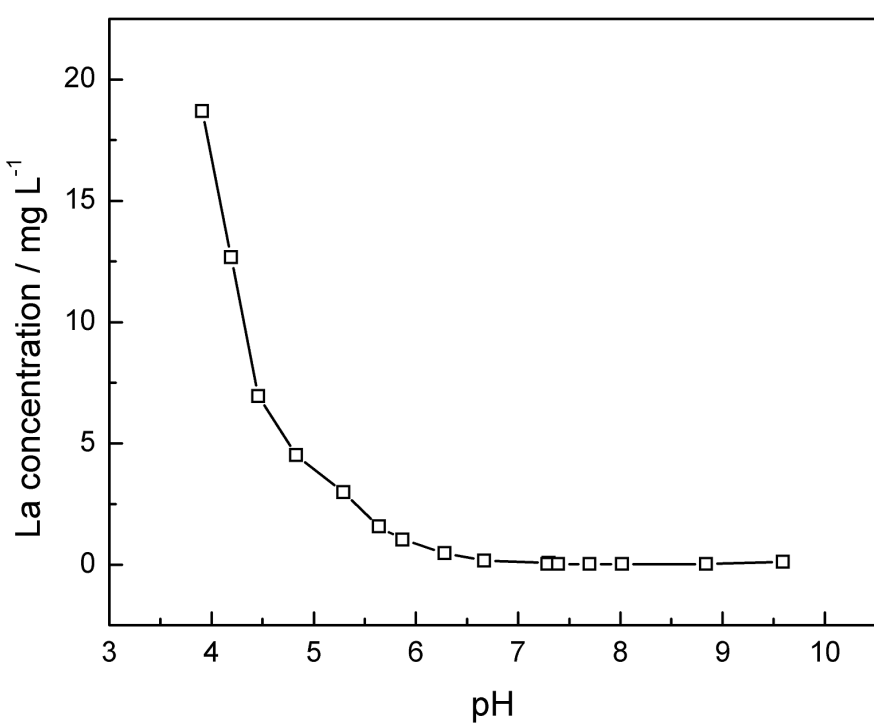


**Fig. S9** La release from LAA as a function of solution pH.

318

319

320

321

322

323

324      References:

- 325      1. C. Y. Jing, J. L. Cui, Y. Y. Huang and A. G. Li, *Acs Appl Mater Inter*, 2012, **4**, 714-720.  
326      2. M. Newville, *J Synchrotron Radiat*, 2001, **8**, 322-324.  
327      3. B. Ravel and M. Newville, *J Synchrotron Radiat*, 2005, **12**, 537-541.  
328      4. T. Luo, J. L. Cui, S. Hu, Y. Y. Huang and C. Y. Jing, *Environ Sci Technol*, 2010, **44**, 9094-9098.  
329      5. J. J. Du and C. Y. Jing, *J Phys Chem C*, 2011, **115**, 17829-17835.  
330      6. M. Newville, P. Livins, Y. Yacoby, J. J. Rehr and E. A. Stern, *Phys Rev B*, 1993, **47**, 14126-14131.  
331      7. J. M. Deleon, J. J. Rehr, S. I. Zabinsky and R. C. Albers, *Phys Rev B*, 1991, **44**, 4146-4156.  
332      8. S. D. Yao, Y. Zheng, L. H. Ding, S. Ng and H. Yang, *Catal Sci Technol*, 2012, **2**, 1925-1932.  
333      9. L. Armelao, G. Bottaro, G. Bruno, M. Losurdo, M. Pascolini, E. Soini and E. Tondello, *J Phys  
Chem C*, 2008, **112**, 14508-14512.

335

336